Phase Transition and Acoustic Localization in Arrays of Air-Bubbles in Water

Zhen Ye* and Haoran Hsu
Department of Physics and Center for Complex Systems, National Central University, Chungli, Taiwan, ROC
(Feb. 5, 1999)

Wave localization is a ubiquitous phenomenon. It refers to situations that transmitted waves in scattering media are trapped in space and remain confined in the vicinity of the initial site until dissipated. Here we report a phase transition from acoustically extended to localized states in arrays of identical air-filled bubbles in water. It is shown that the acoustic localization in such media is coincident with the complete band gap of a lattice arrangement of the air-bubbles. When the localization or the band gap occurs, a peculiar collective behavior of the bubbles appears.

71.55.J; 43.20. *Keywords:* Acoustic localization, Phase transition

Under appropriate conditions, multiple scattering of waves leads to the interesting phenomenon of wave localization, which has been and continues to be a subject of substantial research(e. g. Refs. [1–4]). It has been shown [1] that localization can be achieved for acoustic waves propagation in liquids with even a very small fraction of air-filled spherical bubbles. It is shown that the localization appears within a range of frequency slightly above the natural resonance of the individual air bubbles. Outside this region, wave propagation remains extended.

Multiple scattering and Bragg refraction of acoustic waves in periodic structures can also lead to what has been called a 'complete band gap', which is another fascinating research subject [5]. In the gaps, no wave can propagate in any direction, a useful feature for noise isolation. In this paper we mainly consider acoustic wave localization in random arrays of air-bubbles in water and its possible connections to the complete band gaps of a crystal array of these air-bubbles. We show a coincidence between the localization and the complete band gap in such bubbly liquids. A novel phase diagram is used to characterize the phase transition from the extended to localized states. When the phase transition occurs, an interesting coherent behavior appears.

Consider sound emission from a unit acoustic source located at the center of a bubble ensemble. The acoustic source transmits a monochromatic wave of angular frequency ω. Total number N spherical bubbles of the same radius a are either randomly placed in water or placed regularly to form a simple cubic lattice with lattice constant d. In either cases, the bubble volume fraction, the space occupied by bubbles per unit volume, is the same and taken as $\beta(= a^3/d^3)$. The coordinates of the bubbles are denoted by $\vec{r}_i$ with $i = 1, 2, \ldots, N$. The wave transmitted from the source propagates through the bubbly structure, where multiple scattering incurs, and then it reaches a receiver located at some distance from the bubble ensemble. The multiple scattering is described by a set of self-consistent equations [6] and can be solved rigorously [7].

It is found that the localization of acoustic waves is reached when the bubble volume fraction β is greater than a threshold value of 10^{-5} and the localization behavior is insensitive to the bubble size when the bubble radius is larger than 20 μm [7]. Note that for smaller bubbles, the thermal and viscosity effects are significant enough that the wave localization seems less evident. In the simulation, we take $\beta = 10^{-3}$, and the total number of bubbles is varied from 100 to 2500, large enough to eliminate possible effects on localized states due to the finite sample size. The radius of the bubbles ranges from 20 μ to 2 cm.

The scattered wave from each bubble is a linear response to the direct incident wave p_0 from the source and also *all* the scattered waves p_s from other scatterers, and is written as [7]

$$p_s(\vec{r}, \vec{r}_i) = f_i \left(p_0(\vec{r}_i) + \sum_{j=1, j\neq i}^{N} p_s(\vec{r}_i, \vec{r}_j) \right) G_0(\vec{r} - \vec{r}_i), \tag{1}$$

where f_i is the scattering function of a single bubble, and $G_0(\vec{r}) = \exp(ikr)/r$ is the usual 3D Green's function with k being the usual wavenumber. The total wave $p(\vec{r})$ at any space point is the summation of the direct wave from the transmitting source and all the scattered waves. The scattering function f_i can be readily computed and the solution can be written in the form of a modal series, representing various vibrational modes of each spherical bubble. In the frequency range considered, the pulsating mode dominates the scattering. To solve for $p_s(\vec{r}_j, \vec{r}_i)$ and subsequently $p(\vec{r})$, we set $\vec{r}$ in Eq. (1) to one of the scatterers other than the i-th bubble. Then Eq. (1) becomes a set of closed self-consistent equations which can be solved exactly by matrix inversion. We define $I =< |p|^2 >$ to represent the squared modulus of the total waves, corresponding to the total energy.

A set of numerical experiments has been carried out for various bubble sizes, numbers, and concentrations. Fig. 1 presents one of the typical results of the total wave transmission as a function of frequency in terms

of ka for one random configuration of the bubble cloud. As shown, the transmission is greatly reduced roughly between 0.016 and 0.08 in ka, indicating the localization regime. Note that a few peaks appear below the localization regime. The peak at the lowest frequency is attributed to the effect of finite sample size, and will gradually disappear as the sample size is enlarged. The peak closest to the localization regime is due to the resonance of a single bubble embedded in the ensemble.

Upon incidence, each air-bubble acts effectively as a secondary pulsating source. The scattered wave from the i-th bubble ($i = 1, 2, 3, ..., N$) is regarded as the radiated wave, and can be rewritten as $A_i G_0(\vec{r} - \vec{r}_i)$. The complex coefficient A_i is computed incorporating *all* multiple scattering effects. Express A_i as $|A_i| \exp(j\theta_i)$ with $j = \sqrt{-1}$ here; the modulus A_i represents the strength, whereas θ_i the phase of the secondary source. We assign a two dimensional unit vector $\vec{u}_i$, hereafter termed phase vector, to each phase θ_i, and these vectors are represented on a phase diagram parallel to the $x - y$ plane. That is, the starting point of each phase vector is positioned at the center of individual scatterers with an angle with respect to the positive x-axis equal to the phase, $\vec{u}_i = \cos\theta_i \hat{x} + \sin\theta_i \hat{y}$. Letting the phase of the initiative emitting source be zero, i. e. the phase vector of the source is pointing to the positive x-direction, numerical experiments are carried out to study the behavior of the phases of the bubbles and the spatial distribution of the acoustic wave modulus. The magnitude of the summation of all phase vectors may represent an order parameter.

Figure 2 shows the phase diagrams of the phase vectors (left column) and the averaged wave distribution as a function of distance from the source (right column). The wave distribution is plotted in arbitrary scale and the uninteresting geometric spreading is removed. Three particular frequencies are chosen below, within and above the localization regime, according to the results of Ref. [7]: $ka = 0.01254, 0.01639$, and 0.1. The dots refer to the three dimensional positions of the air bubbles at $\vec{r}_i = (x_i, y_i, z_i)$, with $i = 1, 2, \ldots, N$. The arrows refer to the phase vectors which are located at the bubble sites and are parallel to the $x - y$ plane. The distance dependence of the total wave is scaled by the sample size $R(\sim N^{1/3}d)$. For the purpose of demonstrating the physical picture in its most explicit way, we have only shown here the phase vectors for 136 bubbles.

We observe that for frequencies below the localization regime, roughly below $ka = 0.016$, there is no obvious ordering for the directions of the phase vectors, nor for the wave distribution. The phase vectors point to various directions; the order parameter is nearly zero. In this case, no wave localization appears, corresponding to the extended state in Fig. 1. These features are shown by the example of $ka = 0.01254$, roughly at the resonance of the single bubble. Due to the finite sample size, an oscillatory wave distribution is observed inside the sample, in agreement with a computation from the mean field theory that regards the bubbly water as a uniform medium.

As the frequency increases, moving into the localization regime, the wave localization and an ordering of the phase vectors becomes evident. The case with $ka = 0.01639$ clearly shows that the wave is localized near the source. In the meantime, all bubbles oscillate completely in phase, but exactly out of phase with the transmitting source; all phase vectors point to the negative x-axis, in parallel to the $x - y$ plane. Such a collective behavior allows for efficient cancellation of propagating waves. The appearance of the collective behavior for localized waves implies existence of a kind of Goldstone bosons incurred in the phase transition. The total wave (energy) decays nearly exponentially along the distance of propagation inside the bubble ensemble, setting the localization length [7]. Outside the sample, the transmission remains constant with distance, as expected. The wave localization and the order in the phase vectors are independent of the outer boundary and *always* appear for sufficiently large β and N.

When the frequency increases further, moving out of the wave localization region, the in-phase order disappears. Meanwhile, the wave becomes non-localized again. This is illustrated by the case of $ka = 0.1$. In this case, the phase vectors again point to various directions and the wave distributes roughly uniformly in space. A further study shows that at this frequency, the multiple scattering is negligible. Each bubble mainly experiences the direct incident wave from the source. Thus the phase of each bubble approximates the phase of the incident wave plus a constant phase from the response function of the bubble. As a result, the bubbles at equal distance from the source have the same phase vectors.

In exploring the relation between the above localization behavior with the band gap of regular bubble arrays, we have computed the band structure of a cubic array of air bubbles following Ref. [5]. The result is shown in Fig. 3. We observe that there is a complete band gap between $ka = 0.017$ to 0.09, which coincides with the localization range shown by Fig. 1. The phase vectors and the energy distribution in this cubic array of bubbles are also plotted in Fig. 4 for the three frequencies chosen above. The similar features appear: outside the gap the phase vectors point to various directions, whereas inside the gap all phase vectors point to the same direction in the opposite of the phase vector of the source. As expected, the energy is extended for frequencies outside the gap and localized inside the gap. The similarity between the cases of the random and ordered arrays implies the same mechanism for both the localization and the complete band gap in such systems, and the phase transition be-

tween extended and forbidden bands is similar to that between non-localization and localization.

An intuitive understanding about the acoustic localization in the bubbly structures may be helped from the following consensus. Imagine that two persons hold a thread. If one person pushes, while the other pulls, the two persons would act completely out of phase. No energy can be transferred from one to the other. In the bubbly liquid case, the state of localized waves shows such a completely out-of-phase behavior, which effectively prevents waves from propagating.

We have demonstrated a new phase transition for acoustic propagation in arrays of air-bubbles in water. The results show that as the phase transition occurs, not only the acoustic waves are confined in the neighborhood of the transmitting source, but an amazing collective behavior of the air bubbles appears. The result suggests a coincidence between wave localization and complete wave band gaps.

Acknowledgments. Discussion and help from Alberto Alvarez and Emile Hoskinson are appreciated. The work received support from National Science Council of ROC.

---

[1] D. Sornette and B. Souillard, Europhys. Lett. 7 (1988) 269.
[2] P. A. Lee and T. V. Ramakrishnan, Rev. Mod. Phys. 57 (1985) 287.
[3] R. Dalichaouch, J. P. Armstrong, S. Schultz, P. M. Platzman, and S. L. McCall, Nature 354 (1991) 53.
[4] R. Martinez-Sala, J. Sancho, J. V. Sanchez, V. Gomez, J. Linares, and F. Meseguer, Nature 378 (1995) 241.
[5] M. S. Kushwaha, Int. J. Mod. Phys. B 10 (1996) 977.
[6] L. L. Foldy, Phys. Rev. 67 (1945) 107.
[7] Z. Ye and A. Alvarez, Phys. Rev. Lett. 80 (1998) 3503.

FIGURE CAPTIONS

Figure 1 Averaged transmission as a function of ka.

Figure 2 Left column: The phase diagram for the two dimensional phase vectors defined in the text for one random distribution of bubbles. Right column: The acoustic energy distribution or transmission, averaged for all directions, as a function of distance away from the source; the distance is scaled by the sample size R. (**Original in Color**)

Figure 3 The acoustic band structure for a simple cubic array of air-bubbles. The complete band gap lies between the two dashed horizontal lines. The plot is rendered in terms of the non-dimensional ka as a function of Bloch vectors.

Figure 4 The phase diagram for the two dimensional phase vectors and the energy distribution, averaged for all directions, for the cubic array of the bubbles which has the same bubble volume fraction as the random case. The lattice constant $d = 1/(\beta)^{1/3}a$. (**Original in Color**)

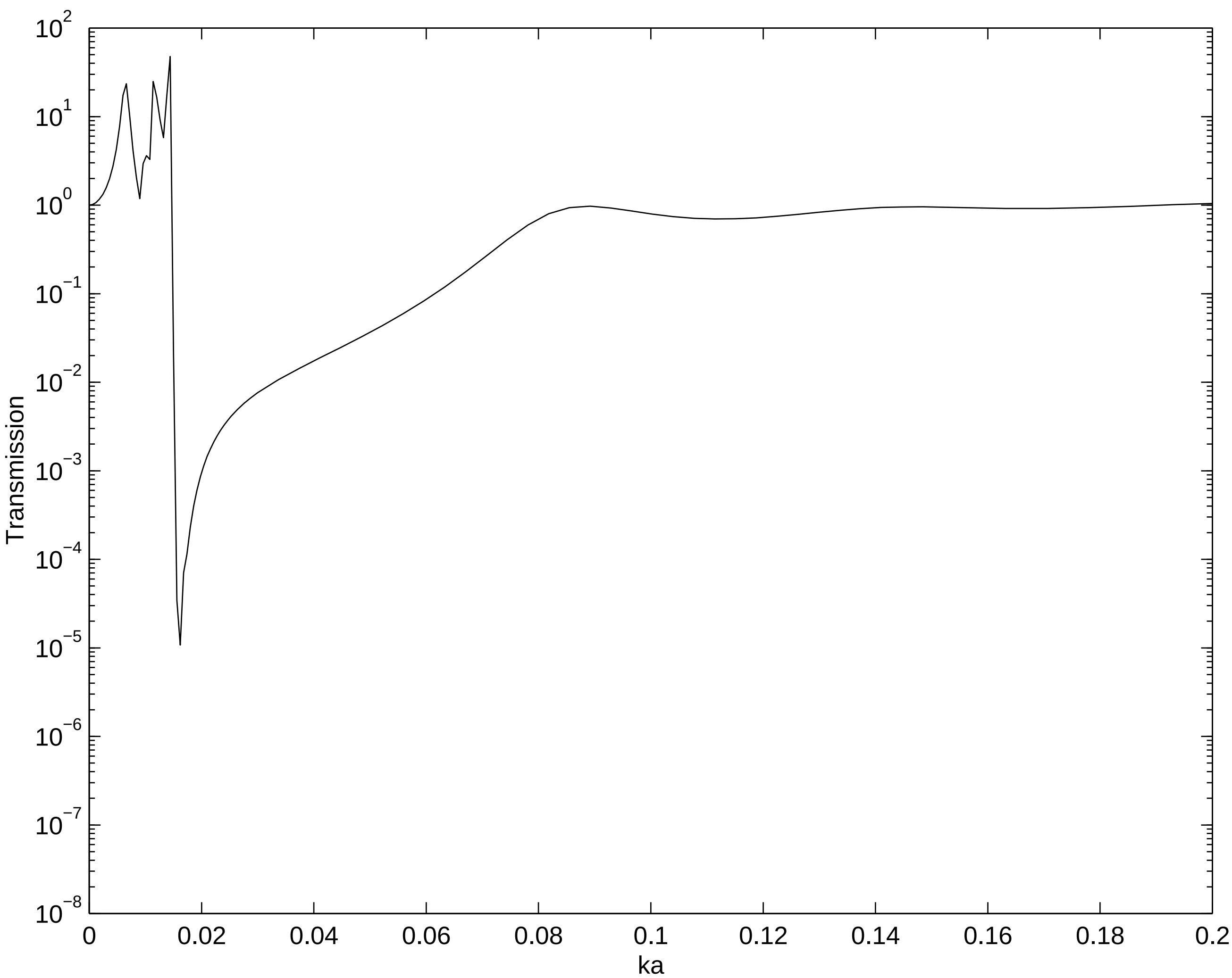

10^2
10^1
10^0
10^-1
10^-2
10^-3
10^-4
10^-5
10^-6
10^-7
10^-8
Transmission
0
0.02
0.04
0.06
0.08
0.1
0.12
0.14
0.16
0.18
0.2
ka

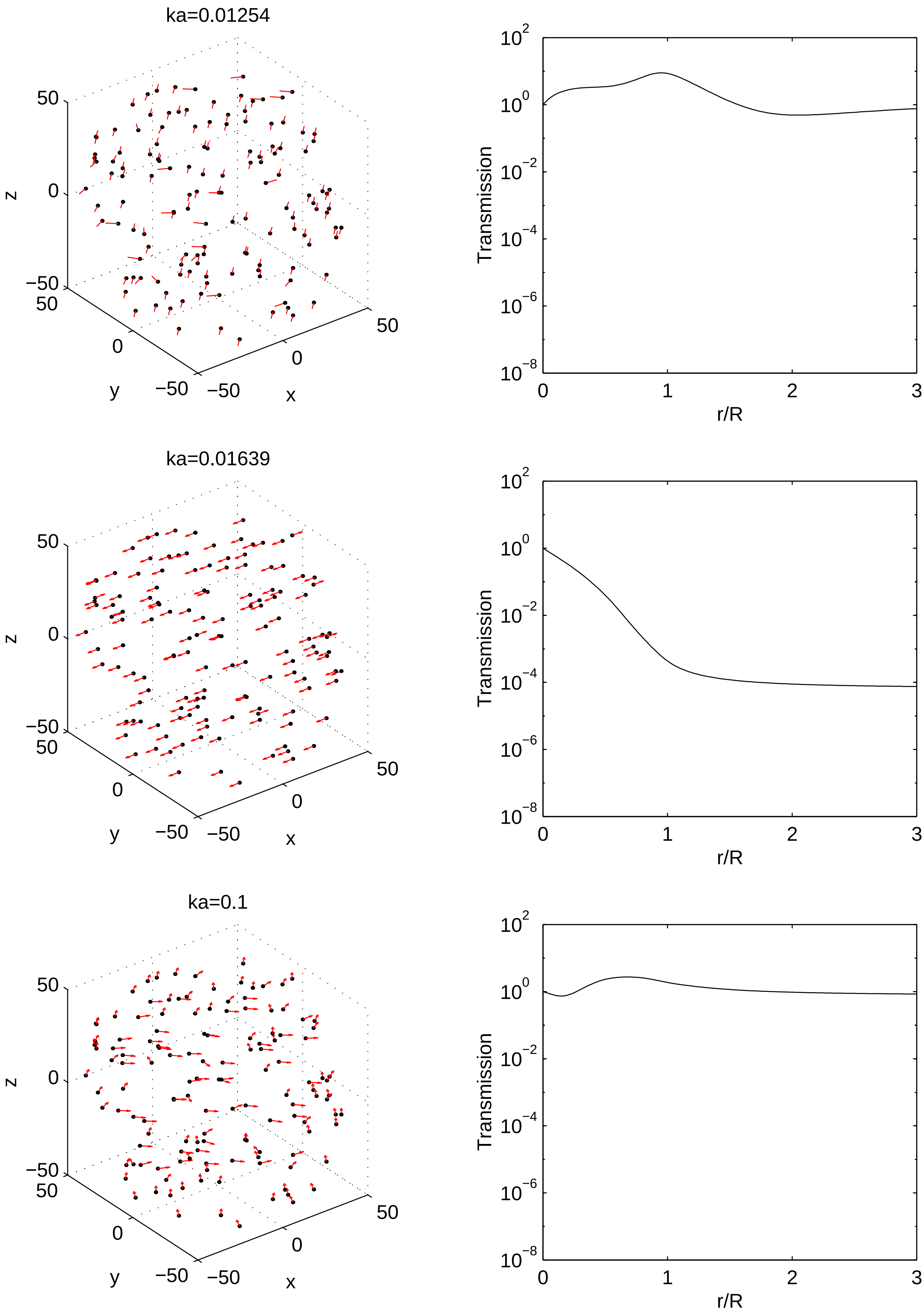

ka=0.01254
ka=0.01639
ka=0.1
x
y
z
50
0
−50
Transmission
r/R
10^{2}
10^{0}
10^{-2}
10^{-4}
10^{-6}
10^{-8}
0
1
2
3

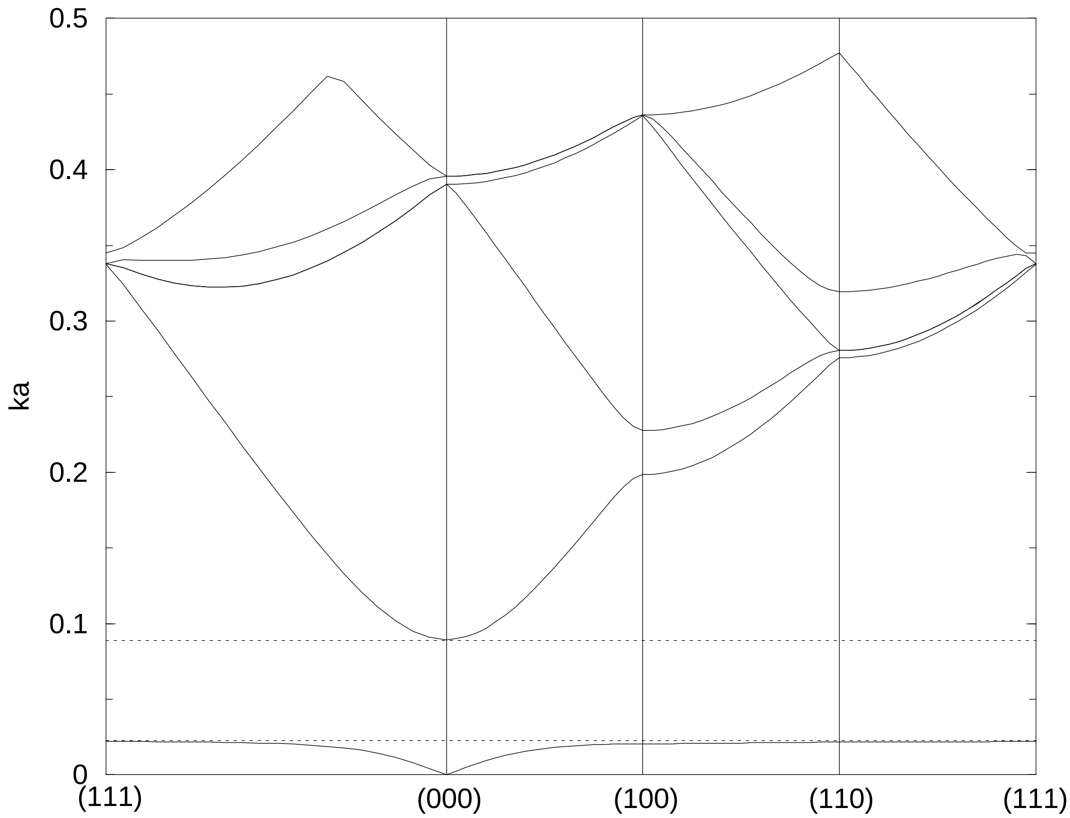

0.5
0.4
0.3
0.2
0.1
0
ka
(111)
(000)
(100)
(110)
(111)

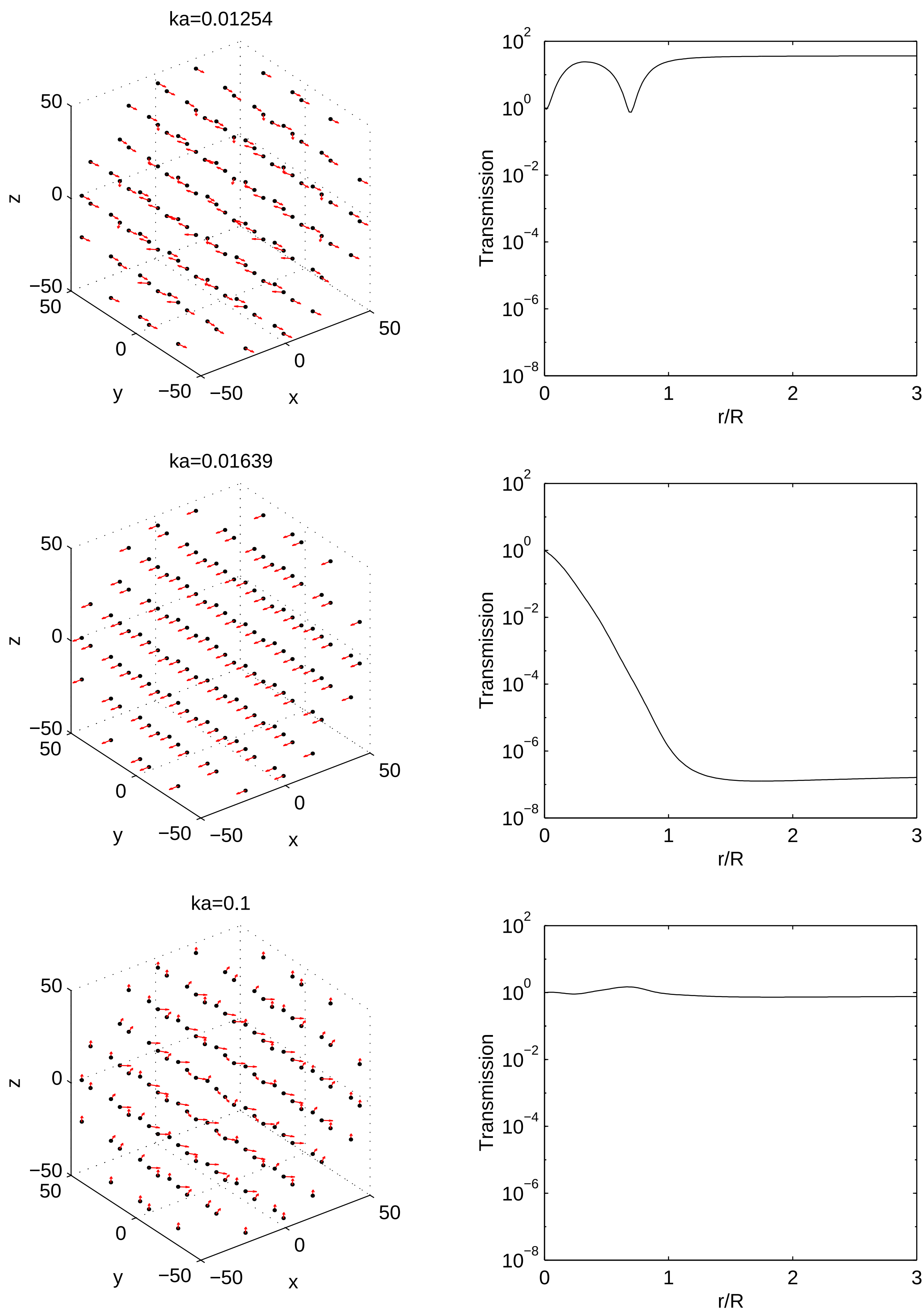

ka=0.01254
ka=0.01639
ka=0.1
x
y
z
50
0
−50
Transmission
r/R
10^{2}
10^{0}
10^{-2}
10^{-4}
10^{-6}
10^{-8}
0
1
2
3